Journal of Alloys and Compounds 509 (2011) 719–723

Contents lists available at ScienceDirect

Journal of Alloys and Compounds

journal homepage: www.elsevier.com/locate/jallcom

Synthesis and characterization of lithium–carbon compounds for hydrogen storage

Hiroki Miyaoka [a], Wataru Ishida [b], Takayuki Ichikawa [a,b,*], Yoshitsugu Kojima [a,b]

[a] Institute for Advanced Materials Research, Hiroshima University, 1-3-1 Kagamiyama, Higashi-Hiroshima, Hiroshima, 739-8530, Japan
[b] Graduate School of Advanced Science of Matter, Hiroshima University, 1-3-1 Kagamiyama, Higashi-Hiroshima, Hiroshima, 739-8530, Japan

ARTICLE INFO

Article history:
Received 3 March 2010
Received in revised form 3 August 2010
Accepted 4 August 2010
Available online 12 August 2010

Keywords:
Nano-structured materials
Mechanochemical processing
Thermochemistry
Calorimetry
Thermal analysis

ABSTRACT

Three carbon materials were prepared for the synthesis of Li–C compounds, such as Li intercalated graphite. The materials were as-received high purity polycrystalline graphite (G), graphite milled under a hydrogen atmosphere (HG), and graphite milled an argon atmosphere (AG). With respect to the difference for them, HG preserved a better crystalline structure than AG. Each material was milled with Li, where the products are denoted as Li-G, Li-HG, and Li-AG. In XRD patterns of Li-G and Li-HG, the peaks corresponding to LiC_6 and LiC_{12} were revealed, while no peaks were observed in the case of Li-AG. However, the formation of lithium carbide Li_2C_2 was suggested for Li-AG by a thermal analysis under an inert gas. After the hydrogenation, LiH was formed for all the compounds, and graphite was recovered for Li-G and Li-HG. Each hydrogenated compound desorbed H_2 with different profile by heating up to 500 °C. As a reaction product, Li_2C_2 was formed for the hydrogenated Li-HG and Li-AG. In the case of the hydrogenated Li-G with better crystalline structure, Li intercalated graphite were formed after the dehydrogenation. Therefore, it is concluded that the hydrogen absorption and desorption process of Li intercalated graphite was different from those of Li_2C_2.

1. Introduction

Carbon materials have been of long interest for energy storage purpose, e.g. hydrogen storage and battery electrode [1–10]. By ball-milling for graphite under H_2 atmosphere, large amount of hydrogen of more than 4 mass% is chemisorbed by the formation of hydrocarbon groups, $–CH_2$ and $–CH_3$, at edges of graphene [11–15], where the hydrogenated graphite is defined as $C^{nano}H_x$. The hydrogenated state of $C^{nano}H_x$ has quite stable C–H covalent bonds, thereby higher temperature than 700 °C is required to release the hydrogen. As another thermal characteristic feature of $C^{nano}H_x$, a large amount of hydrocarbons such as methane CH_4 or ethane C_2H_6 are also desorbed with H_2 desorption. Moreover, it is difficult to recharge the dehydrogenated product with H_2 under moderate temperature and pressure for a practical application. Therefore, plenty of efforts are made to realize pure hydrogen absorption and desorption at modest conditions. Since the report of a new system of $C^{nano}H_x$ and Lithium hydride LiH, it offers a different reaction pathway to desorb hydrogen from $C^{nano}H_x$ by destabilization of C–H bonding via the interaction with LiH [16,17]. Later studies also showed alkali or alkali-earth metal hydrides can reduce the H_2 desorption temperatures and at the meantime, suppress the hydrocarbon release. After H_2 desorption, the nano-structural lithium carbide Li_2C_2 was formed as a reaction product. Li_2C_2 is thermodynamically stable compared with single substances of C and Li, leading to lower H_2 desorption temperatures than $C^{nano}H_x$ and LiH themselves. Furthermore, this product can be recharged with H_2 at 350 °C under 3 MPa of H_2 to form LiH and the C–H bond [18]. This indicates that the reaction path of hydrogen absorption and desorption is changed by the formation of nano-structural Li_2C_2. However, the amount of desorbed hydrogen was gradually decayed after a few cycles of the hydrogen ab/desorption because Li_2C_2 is decomposed into hydrocarbon gas such as methane [19].

As well known, graphite forms intercalated compounds with some alkali metals such as lithium Li and potassium K. Among them, K intercalated graphite provides an alternative way to store hydrogen. Two kinds of compounds with the forms of KC_8 and KC_{24} absorbs 0.49 mass% H_2 by chemisorption at high temperature and 1.2 mass% H_2 by physisorption at low temperature, respectively, by following reactions [20]:

$$KC_8 + 0.335H_2 \rightarrow KC_8H_{2/3} \quad \text{High temperature} \quad (1)$$

$$KC_{24} + 2H_2 \rightarrow KC_{24}H_4 \quad \text{Low temperature} \quad (2)$$

In a similar study, K intercalated super activated carbon (KC_8) was synthesized by thermally treating the mixture with C/K ratio of 4

* Corresponding author at: Institute for Advanced Materials Research, Hiroshima University, 1-3-1 Kagamiyama, Higashi-Hiroshima, Hiroshima, 739-8530, Japan. Tel.: +81 082 424 5744; fax: +81 082 424 5744.
E-mail address: tichi@hiroshima-u.ac.jp (T. Ichikawa).

0925-8388/$ – see front matter © 2010 Elsevier B.V. All rights reserved.
doi:10.1016/j.jallcom.2010.08.002

at 300 °C for 20 h [21]. This compound can absorb 1.6 mass% H_2, greater than H_2 taken by above K intercalated graphite. During the H_2 absorption, the intercalation of K and H_2 into KC_8 leads to the formation of $KC_4H_{0.8}$, with a triple atomic layer of K–H–K between graphene planes. Although the H_2 capacity has been enhanced by synthesis of new K intercalated carbon materials, the involvement of a heavy metal K limits a higher gravimetric capacity of hydrogen.

As mentioned in the earlier part, it was found that the formation of Li_2C_2 as the product on the reaction between $C^{nano}H_x$ and LiH can lead to rechargeable H_2 absorption/desorption. Thereby, it is expected that Li intercalated graphite formed by a high crystalline graphite can store hydrogen rechargeably because it is also thermodynamically stable compound than graphite and Li such as Li_2C_2. In addition, Li can realize higher hydrogen capacity than the K intercalated graphite mentioned above. In this study, the Li intercalated graphite and Li_2C_2 were synthesized from high or low crystalline graphite by ball-milling method, and their hydrogen storage properties were investigated. Finally, difference of the hydrogen absorption and desorption reactions of Li intercalated graphite and Li_2C_2 were discussed.

2. Experimental technique

2.1. Sample preparation

A highly pure graphite powder (99.999%) was purchased from Strem Chemicals, and the sample handling was performed in a glove box (Miwa MFG, MP-P60W) filled with a high purity Ar (99.9999%). Prior to the synthesis of the Li–C compounds, apart from the as-received graphite (G), two kinds of materials were prepared by following methods: (1) a 300 mg G powder was milled under a 1 MPa H_2 in a planetary mill apparatus (Fritsch, P7) with 20 ZrO_2 balls with diameter of 8 mm for 8 h, and the product was denoted as HG; (2) a 300 mg G powder was milled under a 1 MPa Ar in the planetary mill apparatus with the 20 ZrO_2 balls for 8 h, and the product was denoted as AG. Here, the milling pot was made by Cr steel and equipped with a quick connector (Swagelok) to introduce H_2 or Ar gas. Subsequently, a total amount of 900 mg of respective G, HG, or AG and Li granulated metal (99.9%, Aldrich) were milled under Ar for 3 h, where the Li:C ratio was fixed to 1:2, by using the planetary mill apparatus with the 20 ZrO_2 balls to synthesize the Li–C compounds. These Li–C compounds were denoted as Li-G, Li-HG, and Li-AG.

2.2. Experimental procedure

In order to investigate hydrogen absorption properties of the Li–C compounds, differential scanning calorimetry DSC (TA Instruments, Q10 PDSC) was used with two conditions, a 0.5 MPa H_2 flow and a 0.2 MPa Ar flow, up to 500 °C with a heating rate of 10 °C/min. One of the peak temperatures obtained in DSC result under H_2 of each compound was chosen as a temperature for the later hydrogenating treatment. Each compound was treated under 1 MPa H_2 for 12 h in the SUS reactor for a hydrogenation. For the compounds after the hydrogenations, the thermal desorption properties were examined with a heating rate of 10 °C/min. by a combined thermogravimetry (TG), differential thermal analysis (DTA) (Rigaku, TG 8120), and thermal desorption mass spectroscopy (TDMS) (Anelva, M-QA200TS) installed in a glove box, where a high purity He (99.999%) was used as carrier gas. Powder X-ray diffraction XRD (Rigaku, RINT-2100, Cu Kα radiation) was carried out for the samples to identify the reaction products. Then, all samples were covered by a polyimide film (Du Pont-Toray Co. Ltd., Kapton®) in the globe box to avoid an oxidation by exposing to air during measurements. In addition, specific surface area of HG and AG was measured by BET method using N_2 adsorption (Shimazu, Gemini 2375) to characterize the structural properties of them.

3. Results and discussion

In Fig. 1, the XRD patterns of the samples, G, HG, and AG, prepared in advance as the materials of the Li–C compounds are shown. The XRD patterns of G showed clear diffraction peaks corresponding to graphite structure. For HG milled under H_2, the 0 0 2 diffraction peak at around 27° was preserved although its intensity was lowered. On the other hand, AG milled under Ar showed an amorphous-like state, which was mainly due to the graphite fracture through impact by ball-milling. Here, specific surface area of HG and AG was about 500 and 250 cm^2/g, respectively. The specific surface area of AG is twice smaller than HG, suggesting that an agglomeration would occur when graphite is milled in inert

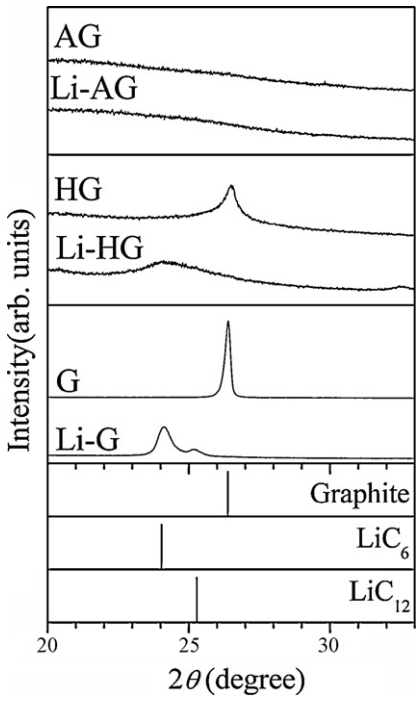

Fig. 1. XRD patterns of the carbon materials and the Li–C compounds. As reference, XRD patterns of Graphite (PDF #41-1487), LiC_6 (PDF #34–1320), and LiC_{12} (PDF #36-1046) in the database are shown.

gas atmosphere. Strictly speaking, the graphene "edges" generated during milling are not terminated by Ar, resulting that the edges form bonding to other carbon atoms randomly. It is expected that the agglomeration leads to the formation of amorphous state [22]. In fact, in the case of ball-milling under H_2, hydrogen atoms are absorbed as hydrocarbon groups such as $-CH_2$ and $-CH_3$ at the graphene edges and defects generated by ball-milling, in other words, the graphene layers were stabilized by the termination of hydrogen atoms [12–15]. The hydrogen absorption on the "edge" site requires lower energy, which would be achieved by the impact of milling under certain H_2 pressures. Meanwhile, Ong and Yang have shown that the milling effect can be minimized when graphite is milled under an O_2 atmosphere [23]. They claimed that the formation of oxides on active centres created during the milling could effectively prevent graphite structure from sliding past one another. So, well crystalline graphite due to large stacking faults can be produced by milling treatment with a reactive atmosphere, in this case, O_2. A similar study carried by Chen et al. also indicates that an increase of H_2 pressure in the milling, which efficiently enhances the H_2 occupancy at the edges of graphite, prevents the fracture of graphite structure during the milling [24]. Therefore, HG shows a better crystallite state with less fracture rate than AG milled under an inert atmosphere of Ar.

The XRD patterns of the Li–C compounds, Li-G, Li-HG, and Li-AG, are also shown in Fig. 1. Li-G synthesized from high crystalline (as-received) graphite G and Li showed continually a better crystalline structure, resulting that Li intercalated graphite, LiC_6 and LiC_{12}, were formed. The HG after milling with Li, Li-HG, showed tendency to be nano-structure although broad peak corresponding to LiC_6 phase were detected. In the case of Li-AG, there is no clear graphite or Li–C compound phases were observed. The difference existing among Li-G, Li-HG, and Li-AG should be caused by the crystallinity of the starting materials. Regarding the formation of Li–C compounds, comparing the intact graphite G, the relatively less crystallinity of graphite might contribute to form the high Li density in graphite layer such as LiC_6 due to more graphene

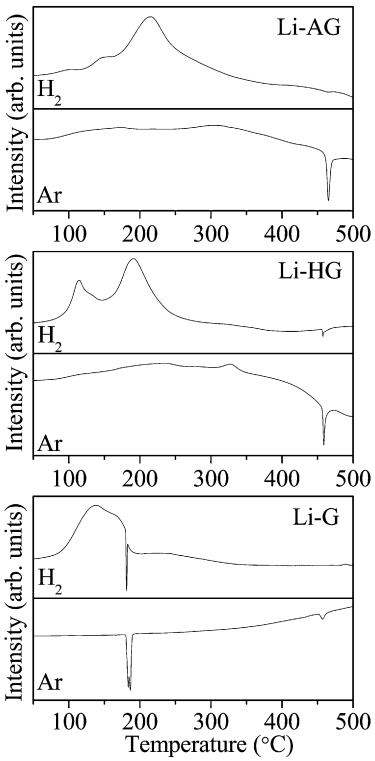

Fig. 2. DSC profiles performed under H_2 (upper) and Ar (lower) atmosphere of the as-synthesized Li–C compounds, Li-G, Li-HG, and Li-AG.

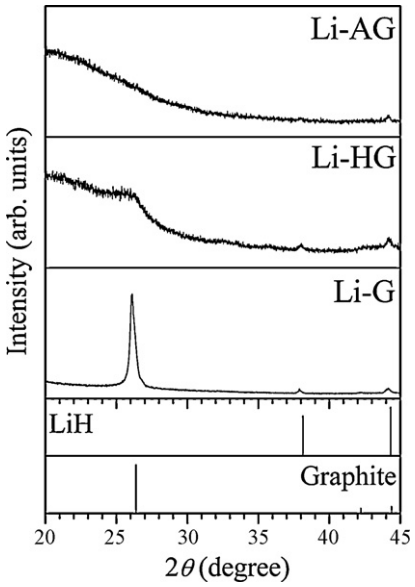

Fig. 3. XRD patterns of Li-G, Li-HG, and Li-AG after the hydrogenation at 140, 190, and 215 °C, respectively. As reference, XRD patterns of graphite (PDF #41-1487) and LiH (PDF #65-9245) in the database are shown.

edges and defects on layers broken by milling. Especially for AG, its already formed amorphous state would as well assist the formation of high density phase LiC_6 or even higher Li-density phase e.g. LiC_2 and Li_2C_2 [25–28]. However, it was difficult to observe these phases with current experimental conditions in this study. In order to identify the Li site in such samples, nuclear magnetic resonance NMR experiment will be useful.

To examine the hydrogen absorption and thermodynamic properties of as-synthesized samples, the DSC measurements were performed under H_2 (for hydrogenation) and Ar (for intercalation) flow condition, respectively. These DSC results of each sample are shown in Fig. 2. In addition, Fig. 3 shows the XRD patterns of each sample after hydrogenation at respective temperature chosen by the DSC measurement under H_2. The DSC profiles of Li-G in Fig. 2 showed a sharp endothermic peak at 180 °C, which is attributed to melting of Li. This is probably due to poor combination of Li with untreated graphite during the milling process. For the DSC results of all the samples under Ar, the same endothermic peaks were observed at around 450 °C. This may be caused by a phase transition of lithium carbide Li_2C_2 [27], suggesting that a nano-structural Li_2C_2 would be formed during milling with Li for all the samples although its amount in Li-G is relatively small. For Li-G under H_2 flow, a broad exothermic peak appeared in the temperature range from 100 to 200 °C. After hydrogenation at 140 °C for Li-G, which is peak temperature in DSC profile, a LiH formation and a recovery of graphite were confirmed by XRD measurements as shown in Fig. 3. The results indicate that the intercalated Li reacted with H_2 and deintercalated to form LiH. Two exothermic peaks appear in the DSC profile of Li-HG as shown in Fig. 2, which may be due to the two different ways to react with H. The first peak at around 120 °C is caused by a reaction of H atoms with the intercalated Li similar to Li-G because the reaction temperature is almost the same. It is expected that the second exothermic reaction at around 190 °C originates in the hydrogenation of the nano-structural Li_2C_2. From these results, the hydrogenation temperature was chosen to be 190 °C for Li-HG. After the hydrogenation treatment, LiH and graphite with low crystallite were formed as shown in Fig. 3. On the other hand, Li-AG showed one broad exothermic peak at around 215 °C. In the XRD pattern after the hydrogenation at peak temperature 215 °C, the diffraction peaks corresponding to LiH was detected, suggesting that nano-structural feature still remained after the hydrogenation treatment. The DSC and XRD results for Li-AG indicate that the hydrogen absorption kinetics of the nano-structural Li_2C_2 is relatively worse than that of the Li intercalated graphite even though both of the compounds can be hydrogenated to form LiH.

TG–TDMS results of the hydrogenated samples and the results of XRD measurements after TG–TDMS are shown in Figs. 4 and 5, respectively. In the TDMS spectra, the intensity of CH_4 is enlarged in ten times. The hydrogenated Li-G sample desorbed only H_2 from 150 °C. A weight loss by H_2 release was about 1 mass% as shown in TG result, suggesting that reversible H_2 capacity of Li-G was about 1 mass%. From the XRD pattern after heating up to 500 °C shown in Fig. 5, it was confirmed that Li was intercalated into the graphite layer again and in addition a small amount of Li_2C_2 was formed. Moreover, non-reacted LiH still remained. The Above experimental facts indicate that Li-G possesses the two different dehydrogenation process, which are paths to form the Li intercalated graphite and Li_2C_2. The existence of two pathways would be caused by the inhomogeneous crystallinity of graphite, in other words, the main part is a high crystalline graphite and a small residual part is a low crystalline graphite formed during the milling process to synthesize Li-G. In the case of the hydrogenated Li-HG and Li-AG, almost the same H_2 desorption with very small amount of CH_4 emission were observed as shown in Fig. 4. Regarding CH_4 desorption, it would be originated in the hydrocarbon groups such as $-CH_2$ and $-CH_3$ formed at graphene edges and defects because the hydrogenated graphite $C^{nano}H_x$ desorbs not only H_2 but also CH_4 as reported before. Li-HG should possess such hydrocarbon groups because HG was synthesized by the milling under H_2. For the Li-AG, the active edges and defects in graphite generated by synthesizing AG would be changed to the C–H groups during the hydrogenation. The weight loss of Li-HG was about 3.5 mass%, which should include a contribution of about 1.5 mass% of hydrogen containing in HG [15]. Thus, assuming that small amount CH_4 emission can

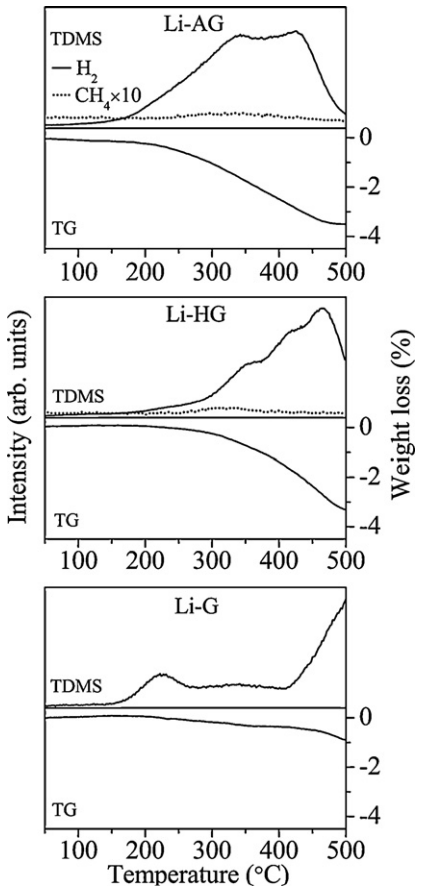

Fig. 4. TG–TDMS results of the hydrogenated Li–C compounds.

be ignored, the essential hydrogen capacity was estimated to be 2 mass%. For Li-AG, the 3.5 mass% of weight loss would correspond to the hydrogen capacity if the contribution of CH_4 emission could be negligible. As shown in XRD patterns of Li-HG and Li-AG in Fig. 5, the diffraction peaks corresponding to LiH phase disappeared after the dehydrogenation. Li_2C_2 was formed as the dehydrogenated state. In previous studies, it is confirmed that $C^{nano}H_x$ with the C–H groups and LiH system can interact with each other to form Li_2C_2 [16,17]. Therefore, the hydrogen desorption properties of the Li–C compounds synthesized from low crystalline graphite would be similar to the $C^{nano}H_x$ and LiH system.

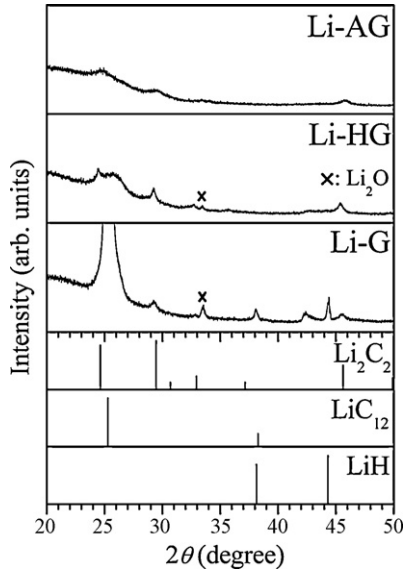

Fig. 5. XRD patterns of the Li–C compounds after TG–MS measurements. As reference, XRD patterns of Li_2C_2 (PDF #21-0484), LiC_{12} (PDF #35-1046), and LiH (PDF #65-9245) in the database are shown.

4. Conclusions

Three types of the Li–C compounds have been synthesized by using the as-received graphite and the pre-milled graphite under different atmosphere, and then their H_2 absorption and desorption properties were investigated from thermodynamic and structural points of view.

In the cases of Li-G and Li-HG, the Li intercalated compounds were confirmed by XRD. However, by DSC measurements under Ar, all three samples show an phase transition of Li_2C_2 at 450 °C, so it suggested that Li-G and Li-HG were composed by Li intercalated graphite and nano-structural Li_2C_2. From thermal analyses by DSC, it was confirmed that the hydrogen absorption process of the Li intercalated compounds and Li_2C_2 were different. The hydrogenation of LiC_6 and LiC_{12} proceeded at lower temperature than Li_2C_2 because of the different kinetic properties. By the hydrogenation, Li intercalated graphite was changed to graphite and LiH. In the case of Li_2C_2, LiH and nano-structural carbon were formed as the hydrogenated state. For the hydrogen desorption properties, dependence on the structural properties was found as well. The high crystalline graphite and LiH in Li-G desorbs only H_2, and Li intercalated graphite was formed again. On the other hand, the part with low crystalline graphite, e.g. Li-AG, revealed the characteristic H_2 desorption properties with the formation of Li_2C_2 by the interaction between the C–H groups and LiH like Li–C–H system [18,19]. As discussed above, the hydrogen storage properties of the Li–C compounds synthesized by the milling would be classified by the crystallinities of starting graphite, which lead to the different reaction process.

From the experimental facts in this work, it was confirmed that H_2 was reversibly stored in the Li intercalated graphite with a repeat of the Li deintercalation and intercalation to graphite below 200 °C as the following equation,

$$C_6Lix + (x/2)H_2 \leftrightarrow 6C(\text{graphite}) + x\text{LiH} \quad (3)$$

Therefore, it was expected that the reversible hydrogen absorption and desorption reactions would be realized because the graphite structure is preserved during each process differently from the Li–C–H system [18,19].

Acknowledgement

This work was partially supported by the NEDO project "Advanced Fundamental Research Project on Hydrogen Storage Materials".

References

[1] A.C. Dillon, K.M. Jones, T.A. Bekkedahl, C.H. Kiang, D.S. Bethune, M.J. Heben, Nature 386 (1997) 377–379.
[2] S. Hynek, W. Fuller, J. Bentley, Int. J. Hydrogen Energy 22 (1997) 601–610.
[3] Y. Ye, C.C. Ahn, C. Witham, B. Fultz, J. Liu, A.G. Rinzler, D. Colbert, K.A. Smith, R.E. Smalley, Appl. Phys. Lett. 74 (1999) 2307–2309.
[4] P. Chen, X. Wu, J. Lin, K.L. Tan, Science 285 (1999) 91–93.
[5] C. Liu, Y.Y. Fan, M. Liu, H.T. Cong, H.M. Cheng, M.S. Dresselhaus, Science 286 (1999) 1127–1129.
[6] C. Park, P.E. Anderson, A. Chambers, C.D. Tan, R. Hidalgo, N.M. Rodriguez, J. Phys. Chem. B 103 (1999) 10572–10581.
[7] A.C. Dillon, M.J. Heben, Appl. Phys. A-Mater. Sci. Process. 72 (2001) 133–142.
[8] A. Züttel, C. Nutzenadel, P. Sudan, P. Mauron, C. Emmenegger, S. Rentsch, L. Schlapbach, A. Weidenkaff, T. Kiyobayashi, J. Alloys Compd. 330 (2002) 676–682.

[9] H. Kajiura, S. Tsutsui, K. Kadono, M. Kakuta, M. Ata, Y. Murakami, Appl. Phys. Lett. 82 (2003) 1105–1107.
[10] M. Hirscher, B. Panella, J. Alloys Compd. 404 (2005) 399–401.
[11] S. Orimo, T. Matsushima, H. Fujii, T. Fukunaga, G. Majer, J. Appl. Phys. 90 (2001) 1545–1549.
[12] K. Itoh, Y. Miyahara, S. Orimo, H. Fujii, T. Kamiyama, T. Fukunaga, J. Alloys Compd. 356 (2003) 608–611.
[13] N. Ogita, K. Yamamoto, C. Hayashi, T. Matsushima, S. Orimo, T. Ichikawa, H. Fujii, M. Udagawa, J. Phys. Soc. Jpn. 73 (2004) 553–555.
[14] T. Fukunaga, K. Itoh, S. Orimo, K. Aoki, Mater. Sci. Eng. B-Solid State Mater. Adv. Technol. 108 (2004) 105–113.
[15] C.I. Smith, H. Miyaoka, T. Ichikawa, M.O. Jones, J. Harmer, W. Ishida, P.P. Edwards, Y. Kojima, H. Fuji, J. Phys. Chem. C 113 (2009) 5409–5416.
[16] T. Ichikawa, H. Fujii, S. Isobe, K. Nabeta, Appl. Phys. Lett. 86 (2005) 241914.
[17] T. Ichikawa, S. Isobe, H. Fujii, Mater. Trans. 46 (2005) 1757–1759.
[18] H. Miyaoka, K. Itoh, T. Fukunaga, T. Ichikawa, Y. Kojima, H. Fuji, J. Appl. Phys. 104 (2008) 053511–053517.
[19] H. Miyaoka, T. Ichikawa, Y. Kojima, Nanotechnology 20 (2009) 204021.
[20] D. Guerard, N.E. Elalem, C. Takoudjou, F. Rousseaux, Synth. Met. 12 (1985) 195–200.
[21] Y. Kojima, N. Suzuki, Appl. Phys. Lett. 84 (2004) 4113–4115.
[22] E. Gomibuchi, T. Ichikawa, K. Kimura, S. Isobe, K. Nabeta, H. Fujii, Carbon 44 (2006) 983–988.
[23] T.S. Ong, H. Yang, Carbon 38 (2000) 2077–2085.
[24] D.M. Chen, T. Ichikawa, H. Fujii, N. Ogita, M. Udagawa, Y. Kitano, E. Tanabe, J. Alloys Compd. 354 (2003) L5–L9.
[25] D. Guerard, A. Herold, Carbon 13 (1975) 337–345.
[26] S. Yata, Y. Hato, H. Kinoshita, N. Ando, A. Anekawa, T. Hashimoto, M. Yamaguchi, K. Tanaka, T. Yamabe, Synth. Met. 73 (1995) 273–277.
[27] U. Ruschewitz, R. Pottgen, Z. Anorg. Allg. Chem. 625 (1999) 1599–1603.
[28] R. Janot, J. Conard, D. Guérard, Carbon 39 (2001) 1931–1934.